Macroporous hybrid Pickering foams based on carbon nanotubes and cellulose nanocrystals

Jean Bruno Mougel, Patricia Bertoncini, Bernard Cathala, Olivier Chauvet, Isabelle Capron

Macroporous hybrid Pickering foams based on carbon nanotubes and cellulose nanocrystals

*Jean Bruno Mougel, Patricia Bertoncini, Bernard Cathala, Olivier Chauvet and Isabelle Capron**

Abstract

The association of nanoparticles with complementary properties to produce hybrids is an underestimated way to develop multifunctional original architectures. This strategy is used to prepare simple, low-cost, and environmentally friendly method to fabricate ultra-low density alveolar foam reinforced with carbon nanotubes (CNTs). This paper investigates the ability of cellulose nanocrystals (CNCs) to produce highly stable oil-in-water Pickering emulsions and to efficiently disperse carbon nanotubes in water to form three-dimensional macroporous conductive foam. It is shown that both single-walled carbon nanotubes (SWNTs) and multi-walled carbon nanotubes (MWNTs) are strongly linked to CNCs by non-covalent interactions, preserving the intrinsic properties of both nanoparticles. Homogeneous surfactant-free emulsions with a droplet diameter of 6 µm are produced. Once concentrated, they can form stable high internal phase emulsions. Incorporating CNTs into these CNC-based emulsions was shown to improve their rheological properties. Freeze-drying the concentrated emulsions produces ultra-low density solid foams (14 mg·cm^{-3}) with several levels of porosity controlled by the emulsification step. Loading CNCs with only 2 to 4 wt% of CNTs, decreases the electrical resistivity of the foam to 10^4 Ω.cm in high relative humidity. The mechanical and electrical properties are studied and discussed in light of the resulting specific foam structure.

Keywords: nanocellulose, Pickering emulsion, biobased, conductivity, foam, cellular foam, porous material, open cell structure.

INTRODUCTION

Cellulose is the most widely found biopolymer in nature. It is composed of glucosidic units and occurs as linear chains arranged in oriented semi-crystalline fibrils.[1, 2] Cellulose nanocrystals (CNCs) are solid crystalline particles that arise from preferential hydrolysis of the amorphous regions,[1] resulting in highly crystalline, elongated nanoparticles whose shape varies according to the source. Cotton fibrils yield solid rod-like nanocrystals with reported dimensions ranging from 150 to 200 nm in length and cross-sections ranging from 5 to 22 nm.[3, 4] CNCs have recently attracted much attention for their use as reinforcement materials in nanocomposites,[5] and their use in films, membranes, catalyst support materials, functionalized drug carriers, support for energy devices and as a templating agent is currently being explored.[6-10] This increasing interest is attributed to their wide availability, sustainability, biodegradability, relatively low cost, lightweight, high aspect ratio, hydrophilicity and high mechanical properties, with a Young's modulus of approximately 150 GPa.[11-15] They notably possess a chemically-reactive surface, which provides the possibility of modification via a chemical reaction strategy.[16-18] Moreover, due to their amphiphilic character, CNCs strongly adsorb at the oil/water interface and can therefore be used as emulsion stabilizers.[19, 20] They form particle-stabilized emulsions also known as Pickering emulsions.[21, 22] Pickering emulsions have been the subject of much attention for the last two decades due to their impressive properties, mainly in terms of stability but also because of the low amount of interfacial agent required, the versatility of the particles used and the coverage yield for different mechanical properties, depending on the concentration and aggregation conditions.[23-25] Another attractive aspect of CNCs is their anisotropic shape at the origin of the low-volume fraction required for percolation, and the specific interactions that make gels and self-assembled structures in dilute regimes,[26, 27] allowing the design of materials with tailored properties. On the other hand, the rigidity of the nanocrystal may be a disadvantage for mechanical properties. It thus might be interesting to conjugate the intrinsic properties of the CNCs with the ones coming from a more flexible nanomaterial,.

Currently, thanks to their excellent electrochemical and mechanical properties, carbonaceous matters including graphene, reduced graphene oxide, carbon nanotubes, carbon fibers and porous carbon are regarded as promising electroactive materials for conductive and storage energy systems. [28-31] Among them, Carbon nanotubes (CNTs) are extremely lightweight, good electrical and thermal conductors and possess outstanding mechanical properties (Young's modulus close to 1 TPa) with a high flexibility, they are thus perfect candidates to achieve new materials[32, 33]. However, they tend to aggregate and can not be dispersed in aqueous media.

Rather than using chemicals, the association of two nanoparticles through physical interactions is an efficient means to produce functional agents, thus forming hybrid particles. The surface of hybrid nanoparticles formed by the physical interactions is generally not modified, preserving their respective properties, as was demonstrated in the case of the efficient self-assembly of CNCs and CNTs.[34, 35] More precisely, CNCs promote an excellent dispersion of CNTs in water with yields as high as 70% of dispersed nanotubes. The stability of the dispersion arises from the fact that CNCs have an excellent colloidal stability in aqueous media due to their chemical structure and to their surface that bears negative charges, allowing electrostatic stability. Similarly, CNTs preserve their conductive properties since no chemical modification of the surface is required.[34, 35] An in-depth analysis showed that both assemblies, based on a hydrophobic effect, occur differently: CNCs align themselves along the single-walled carbon nanotube (SWNT) axis, whereas such an alignment is not observed for CNC/MWNT hybrids.[35] This strategy thus combines the templating and functional properties of both nanoparticles.

In order to simultaneously use CNT to functionalize and reinforce biobased materials with controlled architectures, this study compares the ability of both CNC/SWNT and CNC/MWNT hybrids to form stable oil-in-water Pickering emulsions and of their mechanical properties to form cellular foams. A rheological analysis makes it possible to probe the interfacial layer and provides information about the architecture of the interconnected networks. The CNC/CNT association contributes to a

mechanical reinforcement of the foams in comparison to pure CNC-based foams. This architecture is strong enough to maintain the cellular organization upon freeze-drying in order to produce ultra-low-density foams with a percolated system of characteristic pore size.

EXPERIMENTAL SECTION

Materials

Commercially-available HipCO SWNTs were purchased from Unidym (batch P 062) (Sunnyvale, CA, USA) and used as received. Their diameters ranged from 0.8 to 1.2 nm and their lengths from 100 to 1000 nm (according to the manufacturer's specifications). MWNTs were purchased from Nanocyl (NC 7000) (Sambreville, Belgium). Their average diameter and length were 9.5 nm and 1.5 µm, respectively (according to the manufacturer's specifications). CNCs were prepared from Whatman filter paper (grade 20 CHR, VWR). Water was purified with a Milli-Q apparatus (18.2 MΩ.cm). Cyclohexane (anhydrous > 99%; Sigma Aldrich) was used as received as the oil phase.

Dispersion preparation. Cellulose nanocrystals (CNCs) were extracted from cotton linters using a method adapted from Revol et al.[25] Briefly, 7 g of cotton linters were added to 250 mL of distilled water and mechanically stirred for 24 h. Sulfuric acid (H_2SO_4) was added to obtain a final acid concentration of 58% and heated for 20 min at 70°C. The acid hydrolysis was then stopped by diluting the mixture 5-fold with distilled water. The suspension was then centrifuged (10000 rpm, 10 min), dialyzed to neutrality against Milli-Q water, and deionized using mixed bed resin (TMD-8). The final dispersion was sonicated for 20 min, filtered through 5 and 1.2 µm (Whatman), and stored at 4°C. A surface charge density of 0.1 e/nm^2 of half ester sulfate groups at the surface of the CNCs was determined by conductometric titration with a NaOH solution using a conductivity module (Metrohm). The dimensions of the CNCs were investigated on dry samples with transmission electron microscopy. A statistical analysis of 400 nanocrystals gives an average length L=121+/- 39 nm and an

average width W=10+/- 3 nm. It is worth noting that the nanocrystal section is rectangular and that the W value is an average value.

The preparation of CNC/CNT hybrids is discussed in a previous paper.[35] Briefly, CNC suspension was adjusted to 3.8 g/L in pure water. Two mg of SWNTs or 3 mg of MWNTs were added to 3 mL of CNC suspension, followed by cup-horn sonication (Bioblock Scientific, Vibra-cell 75115 operating at 20 kHz) with a power of 0.7 W/mL, for 2.5 h for SWNTs and 1 h for MWNTs. A cooling bath was used at 4°C. A centrifugation step (20000 g, 30 min), was carried out to remove the remaining CNT bundles, and the supernatant was collected. Thermal Gravimetric Analysis measurements revealed that the CNC concentration remained constant after the centrifugation step. CNT concentration was evaluated by optical absorption experiments performed using a Perkin Elmer Lambda 1050 UV/Vis/NIR.

Emulsion preparation and characterization.

The oil-in-water (o/w) emulsions were prepared using cyclohexane and CNC or hybrid dispersions at in presence of 50 mM NaCl to prevent electrostatic repulsion. The CNC concentration in the aqueous phase is adjusted in all cases to a 4 g/L value by using a concentrated CNC suspension. It was previously shown that under these conditions of concentration and ionic strength, a dense monolayer of CNCs stabilized the interface.[20] The oil/water ratio was adjusted to 20/80. A volume of 1.6 mL of cyclohexane was added to 6.4 mL of aqueous suspension in a plastic vial and sonicated at a power level of 50–55J (Q700 sonicator, Qsonica, Newtown, CT, USA) for 20 s (1 s pulse ON, 1 s pulse OFF). The average droplet Sauter mean diameter *D* and diameter distribution were determined using laser light diffraction measurements with a Malvern 2000 granulometer apparatus equipped with a He-Ne laser (Malvern Instruments, UK). The emulsions were visualized by an optical microscope (BX51 Olympus, France) with a SONY XCD SX90CR video. A drop of the resulting Pickering emulsion was diluted ten-fold using distilled water and followed by vortex stirring. A single drop was then poured onto a slide and visualized using a dark field device. The average drop diameter was compared to the one given by granulometry using Image analysis with Image J software.

The coverage was obtained by the ratio of the theoretical maximum surface likely to be covered by the particles, S_p, and the total surface displayed by the oil droplets, S_d:[19]

where $$S_p = N_p L l = \frac{m_p}{h \rho_p} \quad (1)$$ and $$S_d = 4\pi R^2 \times \frac{3V_{oil}}{4\pi R^3} = \frac{3V_{oil}}{R} \quad (2)$$

N_p is the number of CNCs; L, l and h are the length, width and thickness of the interface, respectively, m_p is the mass of CNCs, ρ is the density (1.6 g/cm^3), R is the average drop radius and V_{oil} is the volume of oil included in the emulsion after centrifugation:

$$C = \frac{S_p}{S_d} = \frac{D\ m_p}{6 \rho_p h\ V_{oil}} \quad (3)$$

where D is the drop diameter and V_{oil} is the volume of oil stabilized by m grams of CNCs.

Rheological characterization of the samples was performed using a controlled-strain rheometer (ARES, TA Instruments, USA) equipped with a plane–plane device (60 mm diameter, 1 mm gap). After preparation, 7.5 mL of the emulsion was centrifuged for 3 min at 4000 g. The tube was pierced in order to remove the subphase and the cream poured on the plate of the rheometer for measurement after a 30-minute equilibration. Strain sweep curves were first used to define the linear viscoelastic region that was linear from 0.1 up to 2% deformation for all the samples (see curve in SI). A sequence was then performed that includes a frequency sweep at 25°C (0.08% strain) from 10^{-2} to 100 rad/s and a strain sweep from 0.07% to 100% (6.28 rad/s frequency).

Preparation and characterization of foams. o/w emulsions were first prepared. Similarly to rheological measurements, the emulsions were centrifuged for 3 min at 4000 g with a tilted angle at 90° in order to obtain perpendicular flat surfaces. The tubes were cut with a razor blade and the water in the subphase removed to keep only the cream that is a hydrated concentrated emulsion. The concentrated emulsion was then deposited on the plane surface of a Petri dish, frozen at -18°C for 12 h and then lyophilized for 24 h using a SRK-System Technik GT2 – 90° freeze-dryer. During freeze-drying, the condenser temperature was below −50°C and the vacuum was below 0.1 mbar in

order to remove both water and cyclohexane, leading to a homogeneous monolithic cellulose foam cylinder (diameter: 13.1 ± 0.1 mm; height: 12.5 ± 1.0 mm).

Scanning electron microscopy (SEM) images of foams were visualized after 40 sec of platinum metallization with a JEOL 6400F microscope operating at 5 kV. Pore sizes were measured directly on the images using Image J software on the basis of an average of 50 to 100 measurements on two representative images.

Mechanical properties: Compression stress strain curves were performed on the foam monoliths. The foams were maintained for one week at 57% relative humidity (RH) in saturated NaBr salts. The compression tests were performed in a controlled RH using a DMTA IV (Rheometric Scientific). The Young's modulus was calculated according to: $\sigma=F/A$ and $\varepsilon=(l_0-l)/l_0$, where σ is the stress (Pa), F the applied force (N), A the surface area in contact with the measuring device, ε the strain, l_0 the initial length and l the length when measured. The measurement was stopped before the densification region was reached.

Electrical properties: Since CNTs are electrical conductors, the electrical properties of the foams that we have produced have been measured. Measuring electrical resistivity of foams is a delicate task, even more so for ultra-lightweight foams. The cylindrical foam samples were used for resistance measurements as produced. The monolith was sandwiched between two copper solid electrodes with a constant applied pressure of 1.47 kPa. It was verified that the resistivity was not pressure-dependent between 0.3 to 1.5 kPa. A four-wire device was used for measurements. The resistance was obtained by sourcing the current between 1 nA to 1 µA and measuring the voltage drop in the ohmic regime across the sample. Guarded cables and a high impedance (Keithley SMU 236) source measurement device were used. The resistivity was obtained from the resistance by taking the geometry of the cylindrical monolith into account. Since cellulose is highly sensitive to humidity, foams were kept in a dessicator with different saturated salts for several days before each

measurement in order to stabilize them at a given relative humidity (RH). The following compounds were used: silica gel (RH=0%), CH_3COOK (RH= 23%), NaBr (RH=58%), NaCl (RH=75%), and $BaCl_2$ (RH=90%) in the dessicator.

RESULTS AND DISCUSSION

Emulsion preparation and characterization.

The cellulose nanocrystals (CNCs) used are nanorods (150-nm long and a cross-section of 7 nm) bearing half sulfated ester groups on the surface that prevent aggregation and produce highly stable suspensions in water. CNC/CNT hybrid nanoparticles were prepared by sonication of the CNC dispersion in water with CNT powder and followed by centrifugation to remove the non-dispersed particles (Fig. SI1a-b). Single (SWNT) and multi-walled carbon nanotube (MWNT) sources were used. They vary in dimension: SWNTs are ~1-µm long with a cross-section of 1 nm, whereas MWNTs are 1.5-µm long with a cross-section of 10 nm. This resulted in two types of hybrids: CNC/SWNTs and CNC/MWNTs that showed very similar dispersible properties.[35] Using this process, suspensions of particles in water with a weight fraction in CNTs of up to 10% were reached. In the present study, a final CNT weigh fraction was adjusted to 2 and 4 wt% to allow a well-controlled content of CNT in emulsions and foams and it was calculated to be enough to reach percolation. These hybrid nanoparticles dispersed in 0.05M NaCl were mixed with cyclohexane and ultrasonicated in order to produce emulsions (Fig. SI1c-d).

It was shown in numerous studies that with an energy input such as sonication, possible aggregates of CNCs are removed and CNCs irreversibly adsorb at the oil-water interface to produce Pickering emulsions that can be stored for months or years.[20]

Similarly to pristine CNCs, in all cases, i.e., with SWNTs or MWNTs, such highly stable emulsions were obtained after sonication. Carbon nanotubes are hydrophobic particles and it is known that the

surface chemistry of the particles controls interfacial properties and, consequently, the type of emulsion.[36, 37] This is determined by the relative wettability of the particle in both liquids, the continuous phase being the preferably wetted phase. Hydrophilic CNCs then logically lead to oil-in-water (o/w) emulsions. When hybrids are used, the same o/w emulsions are obtained. It is true that the addition of such a small amount of CNTs does not sufficiently contribute to a surface chemical change capable of inversing the emulsion. Very similar emulsions were then obtained with a very high stability for both systems since they can remain unchanged for several months and even resist centrifugation. Only the color of the emulsions changes from white to homogeneous gray for both SWNTs and MWNTs (Fig. SI1e-f).

Figure 1 shows optical micrographs of emulsions stabilized with native CNCs, compared to CNC/SWNT (4 wt%) and CNC/MWNT (4 wt%) hybrid particles. As revealed in Fig. 1a-c, individual droplets are obtained with a homogeneous distribution. These observations are confirmed by granulometry analysis. The lower panel in Fig. 1 shows that the droplet distribution is monodispersed in all three cases, with an average diameter of 5 to 6 µm. The droplet distribution obtained by image analysis from the optical micrographs (not shown) is in very good agreement with the observations from light scattering. The average diameter of the droplet distribution is reported in Table 1 for CNC-, CNC/SWNT- and CNC/MWNT-based emulsions. There is no significant difference. Furthermore, CNTs are longer than CNCs, well dispersed in water since several CNCs are attached to a CNT, rendering them hydrophilic by physical adsorption, and it has already been shown that long NPs might promote interconnected networks.[38] In the chosen conditions and as shown in Fig. 1, only individual droplets but no bridging phenomenon were visible.

To check if isolated hybrid nanoparticles are present in the water phase, centrifugation was performed at 4000 g for 3 min. Images are shown in Fig. SI 1 g-h. The cream separates from the excess clear water phase. Since no CNCs were detected visually or by TGA in the excess water and hybrids cannot be dispersed in the oil, this suggests that the entire hybrid NPs were adsorbed at the

interface. It should also be pointed out that the emulsions tested totally resisted centrifugation, showing a clear subphase and a logical densification of the cream at the top of the tube but the total absence of coalescence, confirming the excellent stability of the hybrid Pickering emulsions.

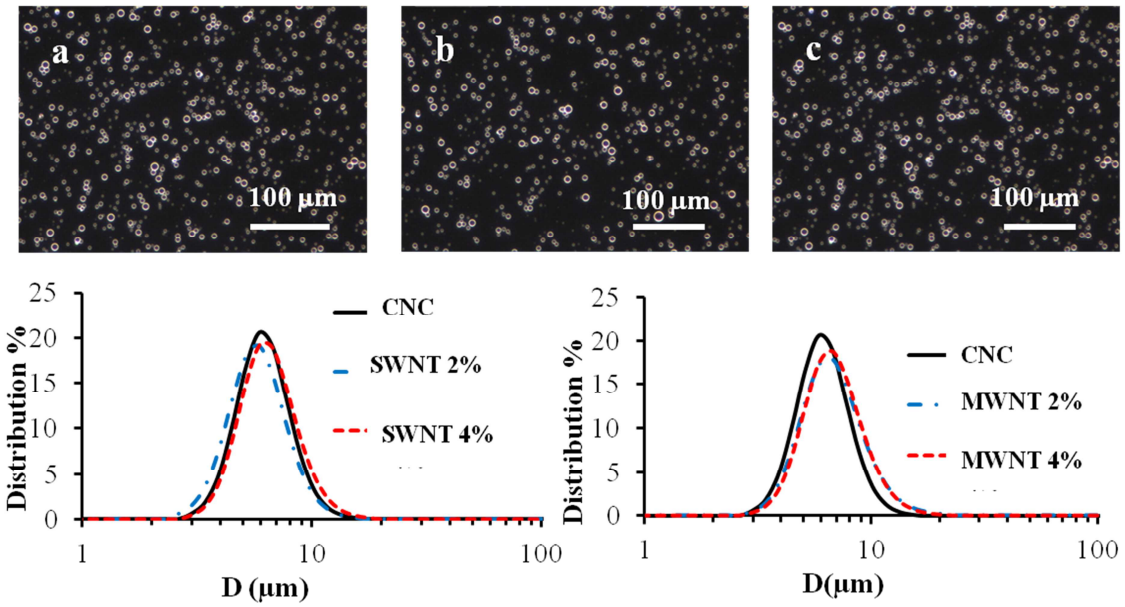

Figure 1: Upper panel: Optical microscopy images of emulsions stabilized with (a) CNCs, (b) 4% CNC/SWNT and (c) 4% CNC/MWNT; Lower panel: droplet size distribution using CNCs alone and compared to (d) CNC/SWNT and (e) CNC/MWNT hybrids at 2% and 4% weight fractions.

The coverage of the droplets by the nanoparticles in the emulsion can be established by the ratio of the interface surface, given by the droplet diameter, and the surface of particles available to stabilize this interface, given by the shape, mass and density of introduced nanoparticles (eq. 1). In the case of pristine CNCs, if it is assumed that the nanocrystals lay flat on the surface, this provides a coverage of 98% for an average droplet diameter of 5.9 µm, i.e., close to a monolayer. This estimation confirms a previous paper in which a neutron scattering study showed that pristine CNCs stabilize the interface by forming a uniform monolayer of 7 nm at the interface.[20] When hybrids are formed, CNCs align themselves along the SWNTs (cross-section of 1 nm). This is not the case with MWNTs, which are

thicker, with an average cross-section (9.5 nm) similar to that of CNCs (10 nm). However, if we assume that 2 wt% or 4 wt% is not high enough to modify the average diameter of the (hybrid) nanoparticle, we find a coverage value C between 93% and 110%. This suggests that the surface is densely covered regardless of the amount of CNTs, 2 wt% or 4 wt%, and that the emulsions are stable for months without coalescence. The same emulsion characteristics are obtained with and without CNTs, which may signify that the CNCs are still responsible for the emulsion stability and that they adsorb onto the interface similarly with and without CNTs.

Physical properties: droplet-droplet interactions

As shown in Fig. 1, the emulsions prepared either with pristine CNCs or hybrid NPs had identical diameter distribution characteristics. Moreover, after centrifugation, the same creaming process occurred. The volume of concentrated emulsions measured in the tube after centrifugation compared to the volume of oil included led to a packing ratio of 0.72. This value is close to the theoretical closest packing of monodispersed spherical particles (0.74) that corresponds to the limit of high internal phase emulsions (HIPE). It indicates both a high resistance to coalescence upon deformation of the interface and a low polydispersity of the droplet diameters. In the case of emulsions stabilized by pristine CNCs, a simple shaking after centrifugation led to the redispersion of the cream in the water continuous phase, as shown in Fig. 2a. Isolated droplets with the same droplet size distribution as before centrifugation were recovered. This is not the case for hybrid stabilized emulsions (regardless of the weight ratio) where droplet aggregation was observed. Figures 2a and 2b illustrate the comparative case of pristine CNCs and CNC/SWNT hybrids. The same behavior was observed for CNC/MWNT hybrids. Mixing the emulsions with a vortex device led to well-redispersed CNC stabilized emulsions, whereas hybrid stabilized emulsions remain cohesive, forming a floating dense cream (see inset in Fig. 2b). Even ultrasound treatment was unable to efficiently separate the aggregated droplets and only very few individual droplets were recovered

(Fig. 2b). This non-reversible aggregation of the droplets is attributed to the presence of CNTs that play the role of a bridge between the droplets. This effect is induced by the centrifugation step that densifies the system. Some differences in the viscoelastic properties of the centrifugated emulsions can therefore be expected.

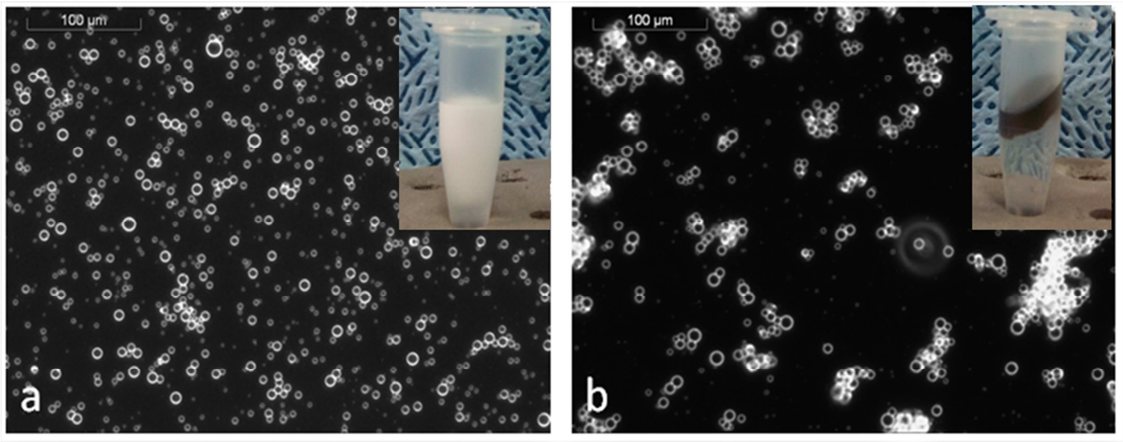

Figure 2: Dark field micrographs of emulsions first centrifuged at 4000 g for 3 min and then redispersed using a vortex for 30 s. (a) Emulsion stabilized with CNCs, and (b) emulsion stabilized with CNC/SWNT hybrids (2 wt%). Inset: photos of the vials after redispersion.

Viscoelastic properties of the emulsions after centrifugation and removal of the excess water were investigated by oscillation measurements. The centrifugation process induces high pressure on the droplets, resulting in concentrated emulsions. As described before, after centrifugation, the droplet diameter is unchanged, but upon relaxation, a new close packing organization is obtained with a volume fraction (ϕ) of 0.72. The frequency dependence of both the storage (or elastic) modulus G' and the loss (or viscous) modulus G'' was measured. The results are shown in Fig. 3 for CNC/SWNT hybrids (left panel) and CNC/MWNT hybrids (right panel). G' reaches a plateau over the measured frequency range, whereas G'' tends to decrease down to a minimum. This last effect, known for emulsions, is more visible at higher concentrations. It is attributed to the droplet caging effect.[39] It reflects droplet rearrangements that slowly relax when the highly concentrated emulsion is

quenched in a glassy structure. On the viscoelastic plateau, CNCs and both CNC/SWNT and CNC/MWNT hybrids show a G' more than one order of magnitude higher than G'' over the entire frequency range. This indicates a predominantly elastic behavior, indicating that a three-dimensional network occurred. The G' and G'' values at f = 6.28 rad/s are reported in Table 1. For a fixed weight fraction of nanoparticles, G' increased notably with the nanotube ratio. For example, including 4 wt% of SWNTs increases the G' value by a factor of 3.5. This is also the case for G" and for tan(δ).

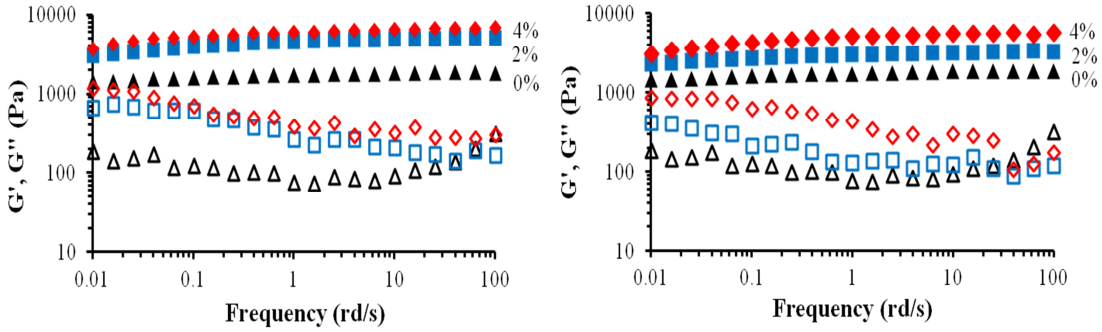

Figure 3: Frequency sweep (γ=0.07%) dependence of storage G' (filled markers) and loss G'' (empty markers) moduli on emulsions stabilized by (i) Left panel: CNC (triangles), 2% CNC/SWNT (squares) and 4% CNC/SWNT (diamonds); (ii) Right panel: CNC (triangles), 2% CNC/MWNT (squares) and 4% CNC/MWNT (diamonds).

Table 1: Average Sauter droplet diameter D, storage G' and loss G'' moduli values at γ= 0.07% strain and f = 6.28 rad/s, half Pascal pressure γ_R, normalized elastic moduli G'/(γ_R) and critical strain γ_{cr} for emulsions stabilized by CNCs, CNC/SNWT or CNC/MWNT hybrids.

	CNC	SWNT/CNC	SWNT/CNC	MWNT/CNC	MWNT/CNC

		2 wt%	4 wt%	2 wt%	4 wt%
Average diameter D (μm)	5.9	5.6	6.2	6.6	6.6
G_p' (Pa)	1800	4900	6300	3100	5400
G_p'' (Pa)	80	200	600	125	400
G'/(γ/R)	0.10	0.27	0.39	0.20	0.36
γ_{cr} (%)	12	39	36	33	33

In order to investigate the interfacial tension contribution to the viscoelasticity of the interface, a comparison with systems stabilized by surfactants can be carried out. The system is at a volume fraction of 0.72, the limit domain above which stress forces the droplets to deform. In such a stable system, no coalescence occurs but the neighboring droplets tend to form flat facets upon constraint. Mason et al. studied monodispersed emulsions stabilized by surfactants.[40] In the case of no attractive interaction between droplets, the elastic modulus (G') is due to the elastic deformation of the droplet shape limited by the interfacial tension. Mason et al. showed that in this situation, G' exhibits a universal volume fraction dependence when normalized by the half Laplace pressure (γ/R) according to the following equation:

$$G' = \gamma/R \cdot f(\phi)$$

where γ is the interfacial tension (50 mN/m for the cyclohexane-water interface), R the radius of the droplet and f(ϕ) a numerical factor that depends on the volume fraction ϕ of the cyclohexane dispersed phase of the emulsion. In the concentrated regime, a good approximation of f(ϕ) is given as $f(\phi) = 1.7\phi^2(\phi - \phi_c)$, which leads to f(ϕ) = 0.075 in our conditions ($\phi = 0.72$; $\phi_c = 0.635$).

We estimated the G' normalized by the half Laplace pressure (γ/R) ratio for the five Pickering emulsions. The results are reported in Table 1. G'/(γ/R) gives a ratio of 0.1 in the case of pristine CNCs that is quite close to 0.075, the "universal" value found for surfactants at the same volume fraction, indicating that the measured G' mainly results from the elastic properties of the droplet oil/water interface without attractive forces between droplets.[41] This result is not surprising since even if counterions are present (50 mM NaCl), isolated droplets were still obtained after several months since CNCs are negatively charged. This results in a behavior very similar to that of highly concentrated emulsions with surfactants. It also suggests that the CNCs alone do not significantly modify the interfacial tension. This is in line with previous results that show no surface tension variation due to CNCs and only a slight reduction of the interfacial tension from 50 mN/m to approximately 45 mN/m at 4 g/L for a dodecane–water interface.[42]

However, when CNC/CNT hybrids are used, the G'/(γ/R) ratio is found to be three to four times higher than the one determined for pure interfacial cyclohexane/water tension. This modification cannot be attributed to γ variation as it would imply γ values above 100 mN/m, which is non-realistic for the present system. Since the droplet dimension variation is negligible, it implies that the increase of the elastic modulus results from an increase of the rigidity of the droplet interfaces due to the presence of the hybrid nanoparticles. In comparison to emulsions stabilized by surfactants, Arditty et al.[41] studied highly concentrated monodispersed Pickering emulsions and proposed that the solid interface may render the droplet surface more rigid. In this case, they proposed to compare G' to ε/R rather than γ/R, ε being an effective elastic coefficient characterizing the droplet surface. With pristine CNCs, the solid-induced rigid character vs. the fluid interface is not predominant since CNCs alone do not increase G'/(γ/R) in comparison to surfactant values. This is not the case in the presence of CNTs. The increase of G' can be attributed to an increased amount of inter-droplet interactions and/or to stronger interactions leading to a more rigid droplet surface. Both effects are likely to play a role. It is probable that adding CNTs promotes a more rigid surface with enhanced lateral attractive interactions. As discussed previously about Fig. 2, centrifuged emulsions can easily be redispersed

when stabilized by CNCs alone, meaning that CNC-CNC interactions do not induce an inter-droplet interaction, whereas this is not the case in presence of CNTs. Such lateral interactions can possibly result from entanglement, newly created van der Waals interactions, capillary immersion forces[43] or any hydrophobic forces resulting from CNT-CNT or CNC–CNT interactions.

The effect is more pronounced for CNC/SWNT hybrids than for CNC/MWNT hybrids. The G' of 1800 Pa for CNCs alone is increased to 4900 Pa and 6300 Pa when SWNTs are integrated at 2 and 4% weight ratios, respectively, compared to 3100 Pa and 5400 Pa in the case of MWNTs at the same 2 and 4% weight ratios, respectively (Table 1).

To validate such a hypothesis, strain sweep measurements were carried out (at f = 6.28 rad/s). The results are shown in Fig. 4. The plateau values at small strains are identical to the ones found by frequency sweeps since they correspond to conditions where the viscoelastic moduli are independent of the applied strain or stress. The G' values increase with the addition of CNT, and a higher increase is observed for SWNTs compared to MWNTs. However a drop in G' and G'' occurs above a critical strain. The critical strain γ_{cr}, defined as the maximum value of G'' is reported in Table 1. It is very close to the intersection between the linear regime of G' at low and high strains. γ_{cr} increases from a 12% strain in the case of pristine CNCs, to 35% in the presence of CNTs, with slightly higher values in the presence of SWNTs than MWNTs. Indeed, this confirms the robustness of the emulsions based on hybrids, which indicates a higher cohesive system in comparison to the emulsions based on CNCs alone. This transition is classically attributed to a collective slipping motion and diffusive entropic relaxation of the unpacked droplet structures. The plateau is also longer for G'' and shows a weak strain overshoot that corresponds to soft glassy materials, which is generally the case for concentrated emulsions.[40] Such strain hardening is normally associated with interconnected network structures like those observed in the case of proteins, for example.[44] An extended linear viscoelastic regime is observed when proteins are cross-linked compared to the

situation with individual components.[45] This leads to the fact that the system is unambiguously stiffer and more interconnected when CNTs are added.

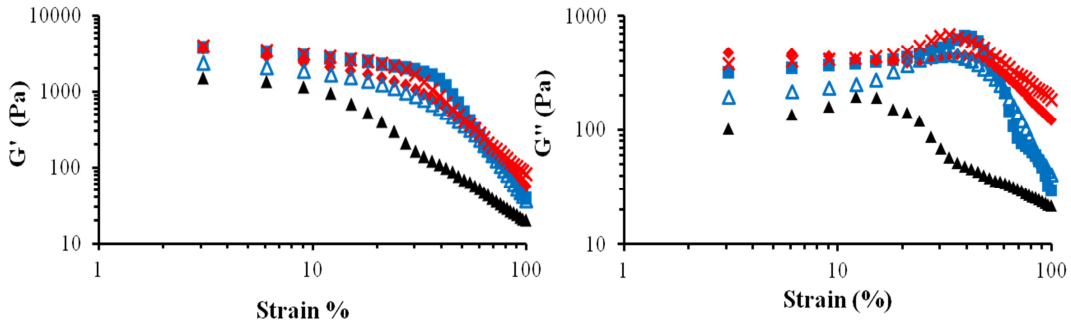

Figure 4: Storage modulus G' (left panel) and loss modulus G'' (right panel) vs. strain (6.26 rad/s frequency) on emulsions stabilized by CNCs alone (filled triangles), 2% CNC/SWNTs (filled squares), 4% CNC/SWNTs (filled diamonds), 2% CNC/MWNTs (empty triangles), 4% CNC/MWNTs (crosses).

Foam mechanical properties and electrical measurements

The highly concentrated emulsions stabilized with solid interface were shown to resist shear when CNCs alone were used.[24] We previously reported that these micron-sized emulsions can support freeze-drying without being disrupted. As illustrated in Fig. 5, the former droplet size distribution of the sample of around 6 µm is preserved during the drying process, revealing that CNC constitutes a strong templating layer, whereas the interface thickness is ultra-low - about 10 nm - forming ultra-low density foam with a cellular macrostructure. The cell size of the foam as measured directly on the SEM images was also the same as the average droplet size of the emulsion when CNTs were added, regardless of SWNTs or MWNTs, at 2 wt% or 4 wt%.

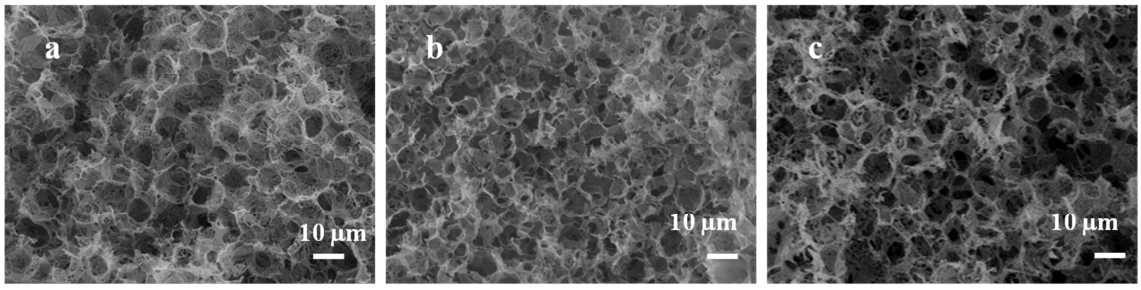

Figure 5: SEM images of cellular foams made of (a) CNCs, (b) CNC/SWNT hybrids, and (c) CNC/MWNT hybrids. The foams were obtained by freeze-drying emulsions stabilized by the nanoparticles mentioned above.

Since adding CNTs increases the storage modulus of the centrifuged emulsions because of a stiffening of the surface and/or the interaction between droplets, it might also increase the mechanical properties of the foam. The compression Young's modulus of the foam monolith was measured using a dynamic mechanical analyzer. The foam samples were prepared in tubes that formed the same cylindrical shape for all samples. Furthermore, since cellulose is sensitive to humidity, they were all conditioned at 57% relative humidity at room temperature prior to compression tests. Typical compression stress–strain curves are shown in Fig. 6. They are composed of two distinct regions: a linear elastic domain at low strain, followed by a plastic domain at higher strain. The Young's moduli (E), calculated as the slope of the initial elastic region, are very low, on the order of 6-7 kPa. However, they increase up to 18 and 29 kPa with the addition of 2 wt% and 4 wt% SWNTs, respectively, as expected considering the viscoelastic properties. In contrast, no better resistance was obtained for MWNTs with a Young's modulus of 6 kPa. This might indicate that there is less cohesion for CNC/MWNT hybrids than for CNC/SWNT hybrids and that more efficient inter-droplet connections were created in the case CNC/SWNT hybrids, whereas this is not the case for the CNC/MWNT hybrids. Even if the mechanical properties are quite low, it is worth noting that only 2 to 4 wt% of SWNTs increases the Young's modulus value three to four times.

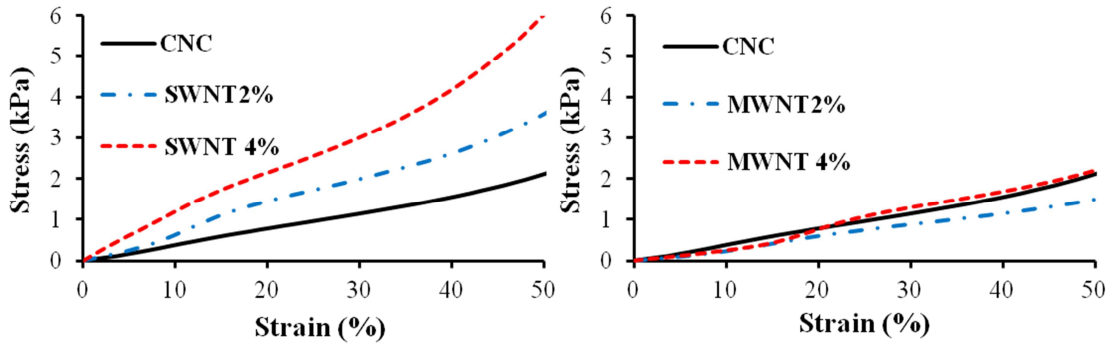

Figure 6: Stress–strain curves obtained on foams built from CNC alone, CNC/SWNT hybrids at 2 wt% and 4 wt% (left panel), and CNC/MWNT hybrids at 2 wt% and 4 wt% (right panel).

The foam density was calculated by weighing and measuring the volume of the freeze-dried samples. They all had a density of 14.0 ± 0.2 mg/cm^3, which is expected since they have the same architecture. This density is smaller or comparable to the density of foams that include CNTs previously reported in the literature (see, for example, references 2-4). The experimental density can be compared to the density calculated by assuming that the foam consists of close packed empty spheres (compacity: 0.74) with a diameter of 6 µm and with 100% coverage of CNCs (density: 1.6 g/cm^3) and a thickness of 10 nm. Such a calculation gives a calculated density of 12 mg/cm^3, which is in very good agreement with the experimental one and corroborates several results: the freeze-drying step does not significantly modify the droplet structure that was created during the centrifugation of the emulsions, the droplets keep their initial size and shape (as confirmed by SEM), and they are covered by a dense (100%) monolayer of CNCs or hybrids.

Comparing this density (0.014 g/cm^3) to the density of CNCs (1.6 g/cm^3) gives a porosity of 99%. This high porosity obviously contributes to quite weak mechanical properties.

Since carbon nanotubes are electrical conductors, it is of interest to evaluate the electrical properties of the foams. As was expected, the resistivity of pure CNC foams is too high to be measured with our set-up. Conversely, the foams with hybrids at 2 wt% or 4 wt% for SWNTs or MWNTs have resistivity values on the order of 10^6 to $10^7\Omega$.cm. This value is too high to consider application. However, it should be recalled that only 1% of the foam volume is solid, and among the solid part, only 2 or 4 wt% are associated with conducting nanotubes. This order of magnitude remains high by comparison to the resistivity of the percolating network of nanotubes in composites, which is usually four to five orders of magnitude smaller.[46] This study revealed that carbon nanotubes localized at the droplet interface form bridges up to a percolating network. This specific architecture of the foam leads to a loose percolating network at very low CNT concentrations.

It is well-known that cellulose, like all polysaccharides, strongly interacts with water molecules. Humidity dependence has already been reported for a similar hybrid system for thin films[34] or on aerogels prepared from CNTs mixed with regenerated cellulose in NaOH–urea aqueous solution.[47] Here, the resistivity was measured for foams stabilized at various relative humidities. As shown in Fig. 7, resistivity increases when the foams are dried, forming insulating foams at low relative humidity. Conversely, increasing the relative humidity drastically decreases the resistivity, which reaches values similar to those reported using modified few-walled carbon nanotubes (FWCNT), for example.[48] In most composites, the presence of humidity usually increases the resistivity because of swelling effects, and such humidity variations are more unusual. When carried out on semi-crystalline materials, water may act as a plasticizer in the amorphous segments (for example, the storage modulus of a film of semi-crystalline nanofibrilated cellulose was shown to decrease with increasing relative humidity).[49] In our case, only the crystalline part of the cellulose remains in the CNCs. Water tends to build a large amount of inter-CNC hydrogen bonds between the hydroxyl groups, reinforcing lateral cohesion. This leads to a better organized and denser network with rubbery characteristics at high moisture contents rather than a rigid network at low moisture contents.

Safari *et al.* reported a study of unbounded NCC/CNT composites for which resistivity increases with the relative humidity whereas it decreased sharply when carboxylated CNC was used.[50] They proposed that the formation of conductive paths on cellulose surfaces through proton hopping is responsible for the sharp decrease of the resistivity when carboxylated CNC was investigated. We cannot neglect such an assumption although we are not using carboxylated CNC. Thus We hypothesize that, as corroborated by our mechanical measurements, in addition to such possibility, increasing relative humidity produces a less fragile and better interconnected network inducing a decrease of resistivity by several orders and, consequently, improving electrical properties.

For the sake of comparison, reports on pure CNT aerogels or PVA-reinforced CNT aerogels prepared using a freeze-drying process.[51] give densities of 10 to 60 mg/cm^3 with an electrical resistivity ranging from 10^2 to 10^7 Ω.cm, depending on the density. Ameli *et al.* prepared polypropylene/MWNT foams using supercritical CO_2,[52] with a relative density ranging from 0.1 to 1 mg/cm^3 and a resistivity between 100 and 10^{13}Ω.cm, depending on the density and the CNT loading.

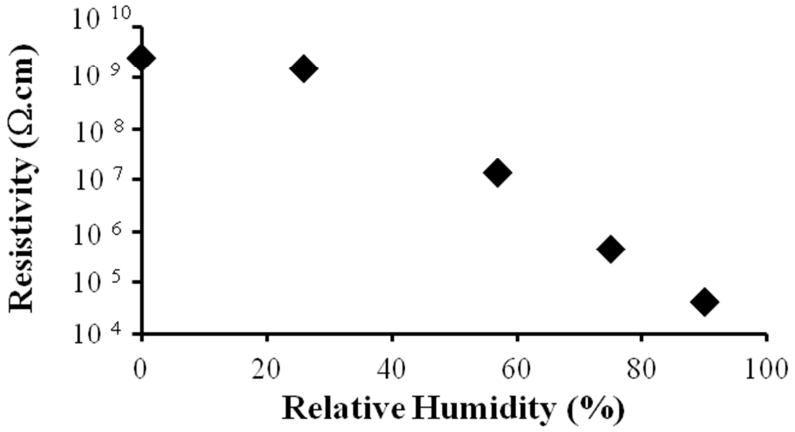

Figure 7: Evolution of the electrical resistivity of a foam monolith vs. relative humidity at room temperature (foam built on 2 wt% CNC/SWNT hybrids)

CNC-CNT hybrids at the interface

The process presented in this work produces ultra-low density foams with a high and controlled porosity (Fig. 8). This process involves CNC/CNT hybrids previously described[34, 35, 53] but used as stabilizers for oil/water Pickering emulsions. The addition of only 2 and 4 wt% CNTs to CNCs contributes to conductivity, simultaneously reinforcing the mechanical properties. This reinforcement is attributed to the stiffening of the droplet surface and new interactions between droplets.

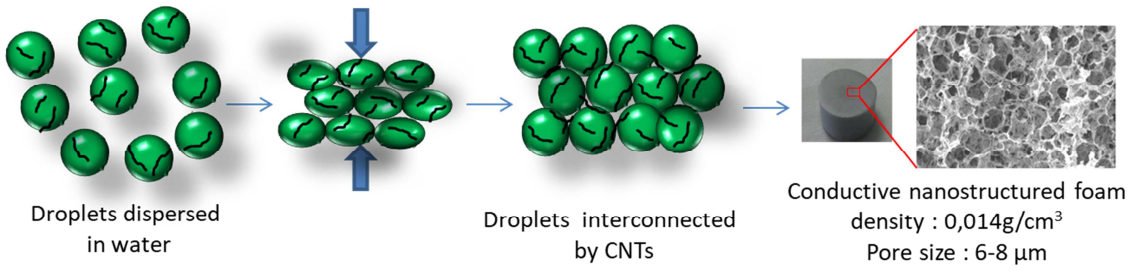

Figure 8: Schematic representation of the conductive foam stabilized by nanohybrid CNC/CTNs. O/W emulsions are prepared and centrifugation forces interactions between CNTs, resulting in lightweight homogeneous foam with porosity controlled by the emulsion process.

Concerning hybrids at the interface, the pristine CNTs alone are unable to stabilize emulsions (furthermore, there is only 2-4% of them), whereas pristine CNCs are able to do so, making it clear that CNCs are the particles that stabilize the interface. As discussed above, when emulsions are formed, no droplet aggregation is observed. However, when emulsions are concentrated by centrifugation up to droplet deformation, contact creates irreversible interactions in the presence of CNTs that are not observed with pristine CNCs (Fig. 8). Such interactions are observed for both types of CNTs but with a significant difference in inter-particle energy, as can be seen by the mechanical results (Fig.6). We previously reported[35] that SWNTs (1 nm thick) tend to align themselves along

CNCs (7 nm thick) with strong interactions repeated all along the CNCs, whereas MWNTs (10 nm thick) are less flexible and do not align themselves along the CNCs. The relative dimensions and possible associations are illustrated in Fig. SI2. Thicker MWNTs result in weaker connections between droplets. This results in a less organized and weaker gel-like 3D system.

Despite these quite strong interactions, the electrical resistivity remains rather high (> 10^4 Ω.cm). A poor dispersion of the fillers may in fact be considered, but this does not seem to be the case, as illustrated by the SEM images in Fig. 9 where foam is visualized without metallization, whereas pure CNC foams, like non-conductive materials, cannot be observed. This shows that the distribution of the CNTs is therefore homogeneous and the percolation threshold is reached, leading to conductive materials for which resistivity is controlled by CNT loading. The quite high level of resistivity may likely to be due to a poor tunnel contact between CNTs arising from the presence of CNC nearby.

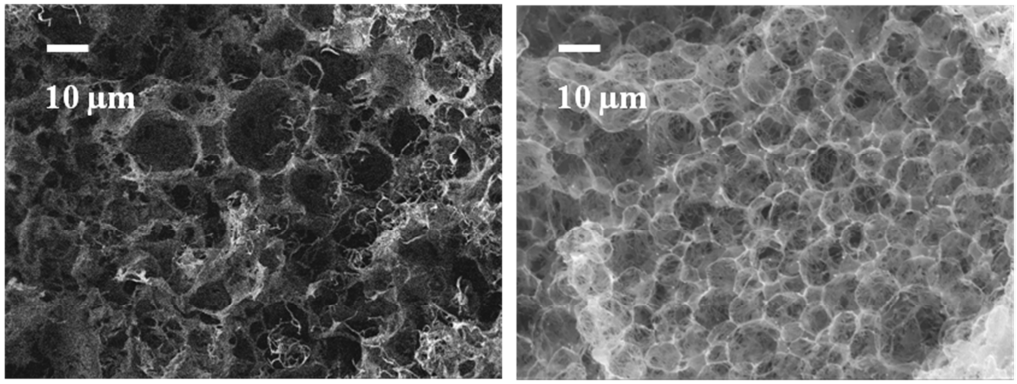

Figure 9: Non-metalized (left) and metalized (right) SEM images of a 2 wt% CNC/SWNT foam. On the right hand side of the non-metalized image, bright filaments associated with conducting SWNTs can be observed. The resolution of the image is poor because of charging effects arising from the insulating CNCs. The metalized image is given for the sake of comparison.

CONCLUSION

On the basis of the previously reported preparative approach, [20, 24, 30-31] this study presents a new way to prepare homogeneous, lightweight, environmental-friendly, macroporous, conductive foams, based on Pickering emulsions. Cellulose nanocrystals are used as biobased templating particles due to their ability to simultaneously associate with conductive carbon nanotubes and to adsorb at the oil-water interface. We show that the physical association that leads to hybrid nanoparticles preserves the intrinsic properties of both CNCs and CNTs. Compared to other works were nanocelluloses are prepared without formation of hybrids that ensure long term stability [48] or mixed without specific organization [54], this study produced 1) highly stable oil-in-water Pickering emulsions with the strong adsorption of SWNT-CNC or MWNT-CNC hybrids at the surface of the droplets, 2) ultra-low density macroporous foams with a pore diameter of approximately 6 µm controlled by the emulsion step via a freeze-drying process without growth of ice crystals due to emulsion templating. Emulsions and foams are mechanically reinforced in the presence of the hybrid nanoparticles. Concerning the aerogels, optical and SEM visualization indicate that the CNTs are homogeneously distributed in the architectures and that the percolation threshold is reached even with only 2 wt% of CNTs. This study therefore proposes a new possibility for the design of highly structured hybrid materials with a low environmental impact, such as conductive lightweight aerogels and films, for final use within a wide range of applications, including batteries, shielding materials and conducting walls, and in the electronics sector.

Acknowledgments

We gratefully acknowledge Nantes University for financial support, Emilie Perrin and Joëlle Davy for their excellent technical assistance for emulsion preparation and SEM visualizations, Genevieve Llamas for granulometry, Catherine Garnier and Camille Jonchère for rheological measurements, and Nicolas Stephant (Institut des Matériaux Jean Rouxel, Université de Nantes) for access to the SEM equipment.

REFERENCES

[1] D. Klemm, F. Kramer, S. Moritz, T. Lindstrom, M. Ankerfors, D. Gray, A. Dorris, Nanocelluloses: A New Family of Nature-Based Materials, Angewandte Chemie-International Edition, 50 (2011) 5438-5466.

[2] R.J. Moon, A. Martini, J. Nairn, J. Simonsen, J. Youngblood, Cellulose nanomaterials review: structure, properties and nanocomposites, Chemical Society Reviews, 40 (2011) 3941-3994.

[3] S. Elazzouzi-Hafraoui, Y. Nishiyama, J.L. Putaux, L. Heux, F. Dubreuil, C. Rochas, The shape and size distribution of crystalline nanoparticles prepared by acid hydrolysis of native cellulose, Biomacromolecules, 9 (2008) 57-65.

[4] F. Cherhal, F. Cousin, I. Capron, Influence of charge density and ionic strength on the aggregation process of cellulose nanocrystals in aqueous suspension, as revealed by small-angle neutron scattering, Langmuir, 31 (2015) 5596-5602.

[5] H. Kargarzadeh, M. Mariano, J. Huang, N. Lin, I. Ahmad, A. Dufresne, S. Thomas, Recent developments on nanocellulose reinforced polymer nanocomposites: A review, Polymer, 132 (2017) 368-393.

[6] C. Martin, B. Jean, Nanocellulose/polymer multilayered thin films: tunable architectures towards tailored physical properties, Nordic Pulp & Paper Research Journal, 29 (2014) 19-30.

[7] K.J. De France, T. Hoare, E.D. Cranston, Review of Hydrogels and Aerogels Containing Nanocellulose, Chemistry of Materials, 29 (2017) 4609-4631.

[8] N. Lavoine, L. Bergstrom, Nanocellulose-based foams and aerogels: processing, properties, and applications, Journal of Materials Chemistry A, 5 (2017).

[9] S. Lombardo, S. Eyley, C. Schutz, H. van Gorp, S. Rosenfeldt, G. Van den Mooter, W. Thielemans, Thermodynamic Study of the Interaction of Bovine Serum Albumin and Amino Acids with Cellulose Nanocrystals, Langmuir, 33 (2017) 5473-5481.

[10] X. Du, Z. Zhang, W. Liu, Y.L. Deng, Nanocellulose-based conductive materials and their emerging applications in energy devices - A review, Nano Energy, 35 (2017) 299-320.

[11] N. Lin, J. Huang, A. Dufresne, Preparation, properties and applications of polysaccharide nanocrystals in advanced functional nanomaterials: a review, Nanoscale, 4 (2012) 3274-3294.

[12] S.J. Eichhorn, A. Dufresne, M. Aranguren, N.E. Marcovich, J.R. Capadona, S.J. Rowan, C. Weder, W. Thielemans, M. Roman, S. Renneckar, W. Gindl, S. Veigel, J. Keckes, H. Yano, K. Abe, M. Nogi, A.N. Nakagaito, A. Mangalam, J. Simonsen, A.S. Benight, A. Bismarck, L.A. Berglund, T. Peijs, Review: current international research into cellulose nanofibres and nanocomposites, Journal of Materials Science, 45 (2010) 1-33.

[13] S. Abend, N. Bonnke, U. Gutschner, G. Lagaly, Stabilization of emulsions by heterocoagulation of clay minerals and layered double hydroxides, Colloid and Polymer Science, 276 (1998) 730-737.

[14] G. Siqueira, J. Bras, A. Dufresne, Cellulosic Bionanocomposites: A Review of Preparation, Properties and Applications, Polymers, 2 (2010) 728-765.

[15] P. Tingaut, T. Zimmermann, G. Sebe, Cellulose nanocrystals and microfibrillated cellulose as building blocks for the design of hierarchical functional materials, Journal of Materials Chemistry, 22 (2012) 20105-20111.

[16] Y. Habibi, Key advances in the chemical modification of nanocelluloses, Chem Soc Rev, 43 (2014) 1519-1542.

[17] S. Eyley, W. Thielemans, Surface modification of cellulose nanocrystals, Nanoscale, 6 (2014) 7764-7779.

[18] M.A. Hubbe, O.J. Rojas, L.A. Lucia, Green Modification of Surface Characteristics of Cellulosic Materials at the Molecular or Nano Scale: A Review, Bioresources, 10 (2015) 6095-6206.

[19] I. Kalashnikova, H. Bizot, B. Cathala, I. Capron, New Pickering Emulsions Stabilized by Bacterial Cellulose Nanocrystals, Langmuir, 27 (2011) 7471-7479.
[20] F. Cherhal, F. Cousin, I. Capron, Structural Description of the Interface of Pickering Emulsions Stabilized by Cellulose Nanocrystals, Biomacromolecules, 17 (2016) 496-502.
[21] B.P. Binks, Particles as surfactants - similarities and differences, Current Opinion in Colloid & Interface Science, 7 (2002) 21-41.
[22] S. Arditty, C.P. Whitby, B.P. Binks, V. Schmitt, F. Leal-Calderon, Some general features of limited coalescence in solid-stabilized emulsions, European Physical Journal E, 11 (2003) 273-281.
[23] C. Salas, T. Nypeloe, C. Rodriguez-Abreu, C. Carrillo, O.J. Rojas, Nanocellulose properties and applications in colloids and interfaces, Current Opinion in Colloid & Interface Science, 19 (2014) 383-396.
[24] S. Tasset, B. Cathala, H. Bizot, I. Capron, Versatile cellular foams derived from CNC-stabilized Pickering emulsions, Rsc Advances, 4 (2014) 893-898.
[25] I. Capron, O.J. Rojas, R. Bordes, Behavior of nanocelluloses at interfaces, Current opinion in colloid and interface science, 29 (2017) 83-95.
[26] M. Chau, S.E. Sriskandha, D. Pichugin, H. Therien-Aubin, D. Nykypanchuk, G. Chauve, M. Methot, J. Bouchard, O. Gang, E. Kumacheva, Ion-Mediated Gelation of Aqueous Suspensions of Cellulose Nanocrystals, Biomacromolecules, 16 (2015) 2455-2462.
[27] K.R. Peddireddy, I. Capron, T. Nicolai, L. Benyahia, Gelation Kinetics and Network Structure of Cellulose Nanocrystals in Aqueous Solution, Biomacromolecules, 17 (2016) 3298-3304.
[28] D.T. Ge, L.L. Yang, L. Fan, C.F. Zhang, X. Xiao, Y. Gogotsi, S. Yang, Foldable supercapacitors from triple networks of macroporous cellulose fibers, single-walled carbon nanotubes and polyaniline nanoribbons, Nano Energy, 11 (2015) 568-578.
[29] H.S. Qi, B. Schulz, T. Vad, J.W. Liu, E. Mader, G. Seide, T. Gries, Novel Carbon Nanotube/Cellulose Composite Fibers As Multifunctional Materials, Acs Applied Materials & Interfaces, 7 (2015) 22404-22412.
[30] G.Y. Chen, T. Chen, K. Hou, W.J. Ma, M. Tebyetekerwa, Y.H. Cheng, W. Weng, M.F. Zhu, Robust, hydrophilic graphene/cellulose nanocrystal fiber-based electrode with high capacitive performance and conductivity, Carbon, 127 (2018) 218-227.
[31] Y.H. Jung, T.H. Chang, H.L. Zhang, C.H. Yao, Q.F. Zheng, V.W. Yang, H.Y. Mi, M. Kim, S.J. Cho, D.W. Park, H. Jiang, J. Lee, Y.J. Qiu, W.D. Zhou, Z.Y. Cai, S.Q. Gong, Z.Q. Ma, High-performance green flexible electronics based on biodegradable cellulose nanofibril paper, Nature Communications, 6 (2015).
[32] Z.C. Tu, Z. Ou-Yang, Single-walled and multiwalled carbon nanotubes viewed as elastic tubes with the effective Young's moduli dependent on layer number, Physical Review B, 65 (2002).
[33] E.W. Wong, P.E. Sheehan, C.M. Lieber, Nanobeam mechanics: Elasticity, strength, and toughness of nanorods and nanotubes, Science, 277 (1997) 1971-1975.
[34] C. Olivier, C. Moreau, P. Bertoncini, H. Bizot, O. Chauvet, B. Cathala, Cellulose Nanocrystal-Assisted Dispersion of Luminescent Single-Walled Carbon Nanotubes for Layer-by-Layer Assembled Hybrid Thin Films, Langmuir, 28 (2012) 12463-12471.
[35] J.B. Mougel, C. Adda, P. Bertoncini, I. Capron, B. Cathala, O. Chauvet, Highly Efficient and Predictable Noncovalent Dispersion of Single-Walled and Multi-Walled Carbon Nanotubes by Cellulose Nanocrystals, Journal of Physical Chemistry C, 120 (2016) 22694-22701.
[36] M. Destribats, S. Gineste, E. Laurichesse, H. Tanner, F. Leal-Calderon, V. Heroguez, V. Schmitt, Pickering Emulsions: What Are the Main Parameters Determining the Emulsion Type and Interfacial Properties?, Langmuir, 30 (2014) 9313-9326.
[37] K. Xhanari, K. Syverud, P. Stenius, Emulsions Stabilized by Microfibrillated Cellulose: The Effect of Hydrophobization, Concentration and O/W Ratio, Journal of Dispersion Science and Technology, 32 (2011) 447-452.
[38] I. Kalashnikova, H. Bizot, P. Bertoncini, B. Cathala, I. Capron, Cellulosic nanorods of various aspect ratios for oil in water Pickering emulsions soft matter, 9 (2013) 952-959.

[39] T.G. Mason, New fundamental concepts in emulsion rheology, Current Opinion in Colloid & Interface Science, 4 (1999) 231-238.
[40] T.G. Mason, J. Bibette, D.A. Weitz, Elasticity of compressed emulsions, Physical Review Letters, 75 (1995) 2051-2054.
[41] S. Arditty, V. Schmitt, J. Giermanska-Kahn, F. Leal-Calderon, Materials based on solid-stabilized emulsions, Journal of Colloid and Interface Science, 275 (2004) 659-664.
[42] Z. Hu, S. Ballinger, R. Pelton, E.D. Cranston, Surfactant-enhanced cellulose nanocrystal Pickering emulsions, Journal of Colloid and Interface Science, 439 (2015) 139-148.
[43] P.A. Kralchevsky, K. Nagayama, Capillary interactions between particles bound to interfaces, liquid films and biomembranes, Advances in Colloid and Interface Science, 85 (2000) 145-192.
[44] L.M.C. Sagis, P. Fischer, Nonlinear rheology of complex fluid-fluid interfaces, Current Opinion in Colloid & Interface Science, 19 (2014) 520-529.
[45] D.Y. Zang, E. Rio, D. Langevin, B. Wei, B.P. Binks, Viscoelastic properties of silica nanoparticle monolayers at the air-water interface, European Physical Journal E, 31 (2010) 125-134.
[46] J.M. Benoit, J.P. Buisson, O. Chauvet, C. Godon, S. Lefrant, Low-frequency Raman studies of multiwalled carbon nanotubes: Experiments and theory, Physical Review B, 66 (2002).
[47] H.S. Qi, J.W. Liu, S.L. Gao, E. Mader, Multifunctional films composed of carbon nanotubes and cellulose regenerated from alkaline-urea solution, Journal of Materials Chemistry A, 1 (2013) 2161-2168.
[48] M. Wang, I.V. Anoshkin, A.G. Nasibulin, J.T. Korhonen, J. Seitsonen, J. Pere, E.I. Kauppinen, R.H.A. Ras, O. Ikkala, Modifying Native Nanocellulose Aerogels with Carbon Nanotubes for Mechanoresponsive Conductivity and Pressure Sensing, Advanced Materials, 25 (2013) 2428-2432.
[49] C. Aulin, J. Netrval, L. Wagberg, T. Lindstrom, Aerogels from nanofibrillated cellulose with tunable oleophobicity, Soft Matter, 6 (2010) 3298-3305.
[50] S. Safari, T.G.M. van de Ven, Effect of Water Vapor Adsorption on Electrical Properties of Carbon Nanotube/Nanocrystalline Cellulose Composites, Acs Applied Materials & Interfaces, 8 (2016) 9483-9489.
[51] M.B. Bryning, D.E. Milkie, M.F. Islam, L.A. Hough, J.M. Kikkawa, A.G. Yodh, Carbon nanotube aerogels, Advanced Materials, 19 (2007) 661-+.
[52] A. Ameli, M. Nofar, C.B. Park, P. Potschke, G. Rizvi, Polypropylene/carbon nanotube nano/microcellular structures with high dielectric permittivity, low dielectric loss, and low percolation threshold, Carbon, 71 (2014) 206-217.
[53] I. Riou, P. Bertoncini, H. Bizot, J.Y. Mevellec, A. Buleon, O. Chauvet, Carboxymethylcellulose/Single Walled Carbon Nanotube Complexes, Journal of Nanoscience and Nanotechnology, 9 (2009) 6176-6180.
[54] L.Q. Zhang, S.G. Yang, L. Li, B. Yang, H.D. Huang, D.X. Yan, G.J. Zhong, L. Xu, Z.M. Li, Ultralight Cellulose Porous Composites with Manipulated Porous Structure and Carbon Nanotube Distribution for Promising Electromagnetic Interference Shielding, Acs Applied Materials & Interfaces, 10 (2018) 40156-40167.

Graphical Abstract